Publication Year	2024
Acceptance in OA	2024-02-21T10:25:34Z
Title	Role of Low-Energy (<20 eV) Secondary Electrons in the Extraterrestrial Synthesis of Prebiotic Molecules
Authors	Wu, Qin Tong, Anderson, Hannah, Watkins, Aurland K., Arora, Devyani, Barnes, Kennedy, PADOVANI, Marco, Shingledecker, Christopher N., Arumainayagam, Christopher R., Battat, James B.R.
Publisher's version (DOI)	10.1021/acsearthspacechem.3c00259
Handle	http://hdl.handle.net/20.500.12386/34799
Journal	ACS EARTH AND SPACE CHEMISTRY
Volume	8

ACS EARTH AND SPACE CHEMISTRY

Open Access
This article is licensed under CC-BY 4.0
http://pubs.acs.org/journal/aesccq

Article

Role of Low-Energy (<20 eV) Secondary Electrons in the Extraterrestrial Synthesis of Prebiotic Molecules

Qin Tong Wu, Hannah Anderson, Aurland K. Watkins, Devyani Arora, Kennedy Barnes, Marco Padovani, Christopher N. Shingledecker, Christopher R. Arumainayagam, and James B. R. Battat*

Cite This: *ACS Earth Space Chem.* 2024, 8, 79–88

Read Online

ACCESS | Metrics & More | Article Recommendations

ABSTRACT: We demonstrate for the first time that Galactic cosmic rays with energies as high as $\sim 10^{10}$ eV can trigger a cascade of low-energy (<20 eV) secondary electrons that could be a significant contributor to the interstellar synthesis of prebiotic molecules whose delivery by comets, meteorites, and interplanetary dust particles may have kick-started life on Earth. For the energetic processing of interstellar ice mantles inside dark, dense molecular clouds, we explore the relative importance of low-energy (<20 eV) secondary electrons—agents of radiation chemistry—and low-energy (<10 eV), nonionizing photons—instigators of photochemistry. Our calculations indicate fluxes of $\sim 10^2$ electrons cm^{-2} s^{-1} for low-energy secondary electrons produced within interstellar ices due to attenuated Galactic cosmic-ray protons. Consequently, in certain star-forming regions where internal high-energy radiation sources produce ionization rates that are observed to be a thousand times greater than the typical interstellar Galactic ionization rate, the flux of low-energy secondary electrons should far exceed that of nonionizing photons. Because reaction cross sections can be several orders of magnitude larger for electrons than for photons, even in the absence of such enhancement, our calculations indicate that secondary low-energy (<20 eV) electrons are at least as significant as low-energy (<10 eV) nonionizing photons in the interstellar synthesis of prebiotic molecules. Most importantly, our results demonstrate the pressing need for explicitly incorporating low-energy electrons in current and future astrochemical simulations of cosmic ices. Such models are critically important for interpreting James Webb Space Telescope infrared measurements, which are currently being used to probe the origins of life by studying complex organic molecules found in ices near star-forming regions.

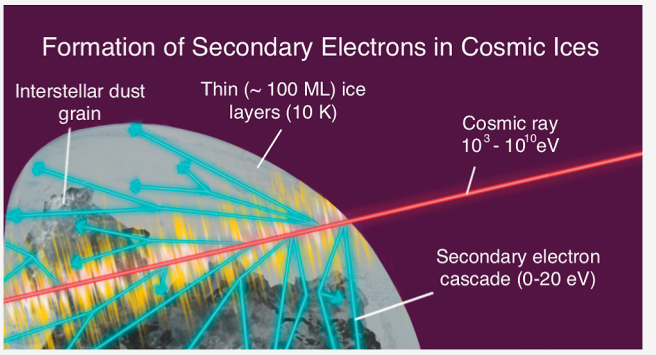

KEYWORDS: *galactic cosmic rays, secondary electrons, interstellar synthesis, prebiotic*

Downloaded via 37.100.234.37 on February 21, 2024 at 10:16:54 (UTC).
See https://pubs.acs.org/sharingguidelines for options on how to legitimately share published articles.

INTRODUCTION

The results of numerous experimental studies provide unambiguous evidence for the low-energy (<20 eV) electron-induced synthesis in interstellar ice analogues of complex organic molecules such as ethylene glycol[1,2] and prebiotic molecules such as glycine, the simplest amino acid.[3] These experiments simulate submicrometer-sized ice mantles surrounding carbonaceous or siliceous dust grains found within interstellar dark, dense molecular clouds, the birthplace of stars. In addition to condensed water, these cosmic ices are composed of ammonia, methanol, carbon dioxide, and other small molecules.[4] These interstellar ice mantles, at temperatures as low as 10 K, are bombarded by Galactic cosmic rays (CRs), which are composed of charged, high-energy particles (e.g., protons, electrons, and helium nuclei) that result from various mechanisms such as particle accelerations during supernova explosions, plasma shocks, or stellar wind collisions.[5] The energetic processing of interstellar ice mantles by high-energy CR particles and ionizing photons (e.g., vacuum UV, X-rays, and γ-rays) is thought to be one of the mechanisms that initiate the extraterrestrial synthesis of prebiotic molecules such as cyanomethanimine (NC_2HNH), which is a precursor of adenine, one of the four DNA nucleobases.[4] In the early stages of our solar system, comets, asteroids, and meteorites carrying these prebiotic molecules may have delivered them to Earth, a likely critical step in the origin of life.[6] The 2022 detection of (1) all the DNA/RNA nucleobases in carbonaceous meteorites[7] and (2) several molecular precursors of RNA in a molecular cloud close to the

Received: September 6, 2023
Revised: November 27, 2023
Accepted: November 29, 2023
Published: December 14, 2023

© 2023 The Authors. Published by American Chemical Society

center of the Milky Way[8] provide tantalizing evidence for this posited mechanism, which is now commonly termed molecular panspermia.

While nonenergetic processing (e.g., thermal chemistry[9] and atom addition reactions[10]) may contribute significantly to the synthesis of prebiotic molecules, our research question involves determining the relative importance of two interstellar ice energetic processing mechanisms: photochemistry and radiation chemistry.[4]

Photochemistry involves chemical processes that occur from the electronically excited state formed by photon absorption; during photochemistry, molecules absorb photon energy but are not ionized.[11,12] Radiation chemistry involves chemical changes produced by the absorption of sufficiently high-energy (typically above 10 eV) radiation to produce ionization.[13,14] Low-energy secondary electrons, the production of which is a signature characteristic of radiation chemistry, are thought to be the dominant species in condensed-phase radiation chemistry.[15] The roles of photochemistry and radiation chemistry in the energetic processing of interstellar ices are depicted in Figure 1.

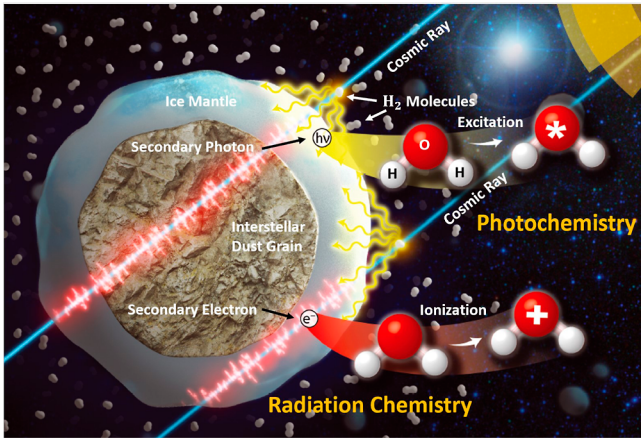

Figure 1. Schematic diagram demonstrating interstellar ices within dark clouds made of molecular hydrogen being processed by photochemistry involving the production of electronically excited water and radiation chemistry involving the production of ionized water and secondary electrons. This work focuses on the interaction depicted in the second of the two CRs (blue lines), in which a CR interacts in the ice mantle to produce secondary electrons. Reproduced from ref 4. Copyright 2019, The Royal Society of Chemistry.

Due to the low temperature characteristic of star-forming regions, most chemical reactions are under kinetic control; reactions with low activation energies are favored. Accordingly, instead of the thermodynamic equilibrium constant, we consider the photolytic/radiolytic dissociation reaction rate constant k, which depends on energy-dependent photon/electron flux $I(E)$ (the number of incident particles per unit time, unit energy, and unit area) and dissociation reaction cross section $\sigma(E)$ (also energy-dependent). As a first approximation,

$$k = \int I(E)\sigma(E)\mathrm{d}E \tag{1}$$

Therefore, we attempt to answer our research question as follows. First, we compare the dissociation reaction cross sections of low-energy electrons and photons. Second, we compare the flux of the Galactic-CR-induced low-energy secondary electrons (the driving force of radiation chemistry) produced within the submicron-sized ice mantles surrounding dust grains to the estimated flux of nonionizing photons (the driving force of photochemistry) incident on interstellar ice mantles.

Even for the simplest of molecules, no experimental data exist to compare directly condensed phase reaction cross sections of low-energy photons and electrons as a function of incident energy. Nevertheless, theoretical considerations suggest that reaction cross sections for electrons should be higher than those for photons.[16] First, due to selection rules, governed primarily by dipole interactions and spin conservation, photon−molecule interactions are more restrictive compared with electron−molecule interactions. For example, unlike electrons, photon-induced singlet-to-triplet transitions are nominally forbidden. Second, in contrast to photons, electrons can be captured into resonant transient negative ion states, which subsequently may dissociate.[16] The resulting molecular fragments may then react with the parent molecule or other daughter products. Importantly, the total cross section for dissociative electron attachment can be several orders of magnitude higher than the geometrical cross section ($\sim 10^{-16}$ cm^2) of a molecule. For example, the total cross section for dissociative attachment is $\sim 10^{-13}$ cm^2 for producing Cl^- from the electron attachment to CCl_4.[17] Third, even though a typical molecule's bond dissociation energy is relatively large (~5 eV), near-zero-energy electrons can cause a molecule to dissociate following electron attachment, especially for molecules that contain elements that have a high positive electron affinity, such as oxygen. Therefore, for incident energies below ~5 eV, the probability for electron-induced dissociation is likely higher than that for photon-induced dissociation because, for a given molecule, photons typically have a higher threshold energy for dissociation. Fourth, the electron attachment cross section for nonpolar molecules increases with decreasing electron energy for very low electron energies (<0.3 meV).[18] Fifth, in contrast to photon impact electronic excitation, direct electron impact electronic excitation (not involving transient anions that decay into excited electronic states) is not an exclusively resonant process; the incident electron transfers a fraction of its energy sufficient to excite the molecule, and any excess is removed by the scattered electron. Because direct electron-impact electronic excitation can operate over a wider range of energies than photon-impact excitation processes, the direct electron-impact contribution to electronic excitation will be greater than any simple comparison of photon and electron-impact excitation cross sections would suggest. Experimental results involving isolated CO molecules on amorphous solid water suggest that electrons are an order of magnitude more efficient than photons in promoting desorption.[19] As a result of the many reasons enumerated above, reaction cross sections are likely larger for electrons than for photons, particularly at incident energies corresponding to resonances associated with dissociative electron attachment.[a]

In addition to electrons having larger reaction cross sections, electron-induced reactions may predominate over photon-induced reactions because of the sheer number of low-energy secondary electrons produced by high-energy irradiation. The interaction between high-energy radiation (e.g., γ-rays, X-rays, electrons, and ion beams) and matter produces copious numbers ($\sim 4 \times 10^4$ per MeV of energy deposited) of cations

https://doi.org/10.1021/acsearthspacechem.3c00259
ACS Earth Space Chem. 2024, 8, 79−88

and nonthermal secondary low-energy electrons.[23] A significant majority of the incident radiation energy is transferred to the kinetic energy of secondary electrons.[24] The inelastic collisions of these low-energy electrons with molecules and atoms produce distinct energetic species that are the primary driving forces in a wide variety of radiation-induced chemical reactions. Therefore, low-energy secondary electrons are thought to be the dominant species in condensed-phase radiation chemistry.[15] Results of Monte Carlo simulations of high-energy radiations interacting with water demonstrate that nearly 90% of the secondary and successive generations of secondary electrons have initial energies less than 20 eV.[25] The most probable energy of the secondary electrons is ∼10 eV.[15] Even though the dissociation probability for a generic molecule increases monotonically with increasing incident electron energy from ∼10 to 100 eV due to dissociative electronic excitation and ionization, the dissociation yield is most significant at low (<20 eV) incident electron energies due to the abundance of secondary electrons at those energies. Figure 2 clearly demonstrates the importance of low-energy (<20 eV) secondary electrons in causing high-energy radiation-induced chemical changes.[16]

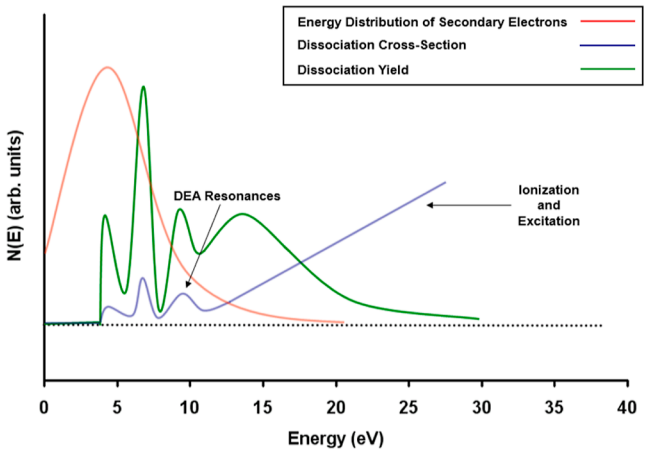

Figure 2. Schematic of the energy distribution of secondary electrons generated during a primary ionizing event (red curve), the cross section for electron-induced dissociation for a typical molecule (blue curve), and the dissociation yield as a function of electron energy for a typical molecule (green curve). The green curve is the product of the red and blue curves. Reproduced from ref 16. Copyright 2009, Elsevier B.V.

Based on the arguments presented above, the primacy of low-energy electrons in the interactions of high-energy radiation with matter is now being exploited for practical applications in disparate fields, suggesting the universality of this phenomenon in radiation chemistry. One such application is cancer treatment.[24,26] Results of quantitative experimental and theoretical studies of low-energy electron-induced DNA lesions are being used to design targeted radionuclide therapy and nanoparticle-aided radiotherapy.[24,27] For example, recent studies suggest that radiation-induced bystander effects may be reduced by exploiting the low mean free path of low-energy electrons emitted by ^{125}I-coated nanoparticles.[28] In addition to their applications in health care, low-energy electrons play an important role in many industrial processes involving ionizing radiation. Recent experimental and theoretical studies have also demonstrated the critical role that low-energy electrons play in extreme ultraviolet (EUV) (92 eV) lithography for the fabrication of next-generation sub-20 nm scale semiconductor chips. For example, electrons with energies as low as 1.2 eV can chemically modify EUV resists, as evidenced by a recent low-energy electron microscopy study.[29] It has long been realized that a fundamental understanding of the production and interactions of low-energy electrons is necessary for optimizing material science techniques such as focused electron beam-induced deposition[30] and plasma processing.[31]

While fields such as cancer therapy and material science have demonstrated tremendous progress in models that incorporate the role of low-energy electrons in the interactions of high-energy radiation with matter, current astrochemical models fail to explicitly account for low-energy secondary electrons produced within cosmic ices by incident high-energy radiation. One notable exception is a recent publication that partially accounts for the role of low-energy secondary electrons in the energetic processing of interstellar ices.[32] Interestingly, in 2018, glycine formation was observed in $CO_2/CH_4/NH_3$ ices irradiated by electrons with energies as low as 9 eV.[3] Low-energy electrons in the interstellar medium may result from two processes: (1) the interaction of Galactic CRs with the gaseous molecular hydrogen present in the dark, dense molecular clouds[33] and (2) the inelastic collisions that ionizing radiation (e.g., Galactic CR) experiences as it traverses through the ice-covered dust grains.[34] Recent calculations indicate that an electron produced through process (1) strikes a dust grain in a dense molecular cloud once every 25,000 years,[31] suggesting that low-energy electrons incident on ices play an insignificant role in interstellar chemistry. However, by focusing solely on incident electrons, these calculations ignore a more significant interstellar ice radiation chemistry driver: low-energy secondary electrons produced within cosmic ices by Galactic CRs and high-energy radiation internal to the molecular cloud. We estimate the flux of Galactic-CR-induced secondary electrons within interstellar ices by (1) considering the attenuated Galactic-CR particle spectra after propagation through dark, dense molecular clouds and (2) using data from the National Institute for Standards and Technology (NIST) PSTAR[b] database to account for the total stopping power (the energy loss per unit length) for protons in water (used as a model for ice, as discussed later). Our results indicate that the flux of Galactic-CR-induced low-energy electrons within interstellar ices is almost as substantial as that of nonionizing UV photons incident on ices in dark, dense molecular clouds.

Attenuated Galactic CRs are not the only source of ionizing radiation incident on interstellar ices within dark, dense molecular clouds. In certain stellar nurseries, the CR ionization rate of molecular hydrogen (hereafter CRIR) has been discovered to be a thousand times greater than typical observed Galactic values of $\sim 10^{-17}$ to 10^{-15} s^{-1}.[35,36] This enhancement in the CRIR has been attributed to embedded ionizing radiation sources within these star-forming regions. This high-energy radiation is likely due to populations of relativistic particles and their associated nonthermal synchrotron emission. Charged particles may be accelerated in protostellar jet shocks and in accretion shocks on protostellar surfaces. Although protostellar jet velocities (tens to hundreds of km s^{-1}) are much smaller than relativistic speeds, these particles reach relativistic velocities through the diffusive shock acceleration mechanism in which particles gain energy by diffusing back and forth across a shock or jet front.[37−40] Recent research has provided evidence to support this incipient

https://doi.org/10.1021/acsearthspacechem.3c00259
ACS Earth Space Chem. 2024, 8, 79−88

theory. For example, observations with the NRAO's Karl G. Jansky VLA of the Class I intermediate-mass protostar HOPS 370 of the Orion molecular cloud 2 located at a distance of 414 ± 7 pc suggest that nonthermal synchrotron emission from relativistic electrons accelerated in shocks produces the observed nonthermal emission from knots (compact regions in molecular clouds where gas and dust are concentrated). Nonthermal synchrotron emission has also been detected in well-known protostellar jets, HH 80−81, located in the L291 cloud in Sagittarius at 1.7 kpc, thus indicating that acceleration mechanisms exist within the jet and may be responsible for the enhanced CRIR.[41] Other deep radio continuum observations at 325 and 610 MHz using the Giant Metrewave Radio Telescope of the young, low-mass star DG Tau located at 140 pc in the Taurus molecular cloud provide tentative evidence for the acceleration of particles to relativistic energies due to the impact of a low-power jet suggesting that low-energy CRs are being generated by young, low-mass stars.[42] Additionally, ALMA observations of the Class 0 protostar object B335 that is associated with an east−west outflow located at 164.5 pc show very high CRIRs (between 10^{-16} and 10^{-14} s^{-1}) that increase toward the central protostellar embryo, indicating that the local acceleration of CRs and not the penetration of interstellar Galactic CRs may be responsible for the gas ionization in the inner envelopes of the protostar.[43] Moreover, observations of FIR4, a young intermediate-mass protocluster of the Orion molecular cloud 2, using the IRAM NOEMA interferometer uncovered a possible jet shock propagating toward a previously measured enhanced CRIR region, suggesting that energetic particle acceleration by jets might be responsible for the enhanced CRIR in these regions.[44] These recent observations suggest that internal high-energy ionizing radiation sources could be a dominant source of low-energy secondary electrons produced within ice mantles found inside dark, dense molecular clouds, the birthplace of molecules and stars.

Observations detailed above and our calculations described herein demonstrate that the flux of low-energy secondary electrons within interstellar ices produced by Galactic CRs and internal ionizing radiation may far surpass that of nonionizing photons incident on interstellar ices. Because electrons likely have larger reaction cross sections than photons, our calculations demonstrate the pressing need for astrochemical models to incorporate the role of low-energy (<20 eV) electrons in the extraterrestrial synthesis of prebiotic molecules.

METHODS

Overview. To compute the number of CR-induced low-energy electrons available for radiation chemistry in cosmic ices, we select a Galactic CR spectrum for protons and then compute how that spectrum is attenuated as the Galactic CRs traverse a molecular cloud composed primarily of molecular hydrogen. The protons in this attenuated Galactic spectrum subsequently interact with ice-covered dust grains, losing energy and producing secondary electrons that can contribute to radiation chemistry. In this section, we describe our choice of model for the initial Galactic CR proton spectrum, the procedure by which we compute the postpropagation spectrum, and the methodology by which we estimate the number of Galactic-CR-induced electrons produced in the ice-covered interstellar dust grains.

Galactic Cosmic Ray Spectrum. Galactic CR particles, with energies as high as 10^{20} eV, consist of approximately 90% protons, 9% alpha particles, and 1% heavier nuclei.[45] While the flux of hydrogen and helium nuclei dominates all other species, there is also a steady flux of CR electrons, positrons, and antiprotons.[46] The total Galactic CR-induced secondary electron flux is the sum of the secondary electron flux produced by CR protons, alpha particles, heavier nuclei, electrons, positrons, and antiprotons. Here, we restrict our calculations to Galactic CR protons. We also ignore secondary electrons produced by ionizing vacuum UV, γ-rays, and X-rays incident on ices within dark, dense molecular clouds. Most importantly, we do not take into account embedded ionizing radiation sources within star-forming regions inside molecular clouds. Therefore, our calculations represent a lower bound to the secondary electron flux produced by ionizing radiation within interstellar ices, and yet, we still find that the electron flux is significant.

The spectra of interstellar CR nuclei at high energy (above 1 GeV nuc^{-1}) are well-constrained by ground, balloon, and satellite observations;[47,48] however, the low-energy nuclei are strongly influenced by solar modulation effects, and their spectra are less well-constrained.[49,50] Voyager 1 and 2 data[51,52] provide the best constraints on interstellar CR spectra at low energies.

In this work, we use the analytical model for the interstellar CR spectrum of protons (and electrons) provided by Ivlev et al.[53]

$$j(E) = C\frac{E^{\alpha}}{(E + E_0)^{\beta}} \quad \mathrm{eV^{-1}\,cm^{-2}\,s^{-1}\,sr^{-1}} \tag{2}$$

We adopt the slightly modified parameter values for E_0 and α, as advocated by Padovani et al.[54] The associated model parameter values are given in Table 1, and a plot of the spectra is shown in Figure 3.

Table 1. Parameters for the Interstellar CR Proton Spectrum for Model L and Model H, as Defined in eq 2

species	C	E_0/MeV	α	β
p (model L)	2.4×10^{15}	650	0.1	2.8
p (model H)	2.4×10^{15}	650	−0.8	1.9

We consider two models for the Galactic CR proton spectrum: model L ("low") and model H ("high"). Model L is based on Voyager 1 and Voyager 2 data collected within the very local interstellar medium.[52] The data were obtained when

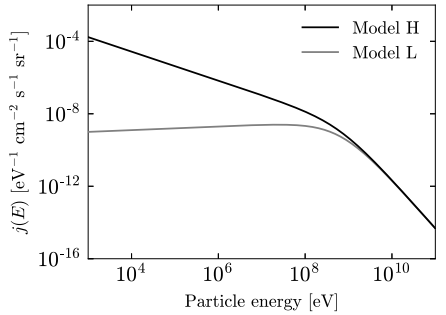

Figure 3. Differential interstellar CR spectra for protons—see eq 2 and Table 1.

https://doi.org/10.1021/acsearthspacechem.3c00259
ACS Earth Space Chem. 2024, 8, 79−88

the spacecraft was at a heliocentric distance of 122 AU, just beyond the heliopause. Although Voyager 1 and Voyager 2 provide the only direct observational constraint currently available on the low-energy CR spectra, the measured proton flux is likely not the interstellar flux because the spacecraft had not yet entered the interstellar space.[53] Most importantly, model L fails to reproduce the CRIR estimated from observations in diffuse clouds.[55] Hence, model H was introduced to ensure agreement with the average ionization rate of H_2, as derived from the measured abundance of H_3^+ in diffuse clouds.[53] Models L and H are taken to be the lower and upper bounds on the proton Galactic CR spectrum, respectively.

Computing the Local Cosmic Ray Spectrum. The interstellar CR spectrum is altered (attenuated) as it propagates through a molecular cloud. Molecular clouds consist primarily of H_2 (molecular hydrogen), with contributions from other species (He, C, N, O, etc.) typically less than 15%. For this work, it is sufficient to approximate the cloud composition as 100% H_2. Future work could consider more detailed interstellar medium compositions, such as those given in Wilms et al.[56]

To model the interactions of the Galactic CR protons with the molecular cloud, we adopted the continuous-slowing-down approximation (CSDA). The CSDA assumes that the proton's direction of propagation does not change significantly from the interactions with the H_2 molecules and that the energy loss function of the proton $L(E)$ is continuous along its path and proportional to dE/dl the energy lost per unit path length l

$$L(E) = -\frac{1}{n(\mathrm{H}_2)}\left(\frac{dE}{dl}\right) \tag{3}$$

where $n(H_2)$ is the number density of molecular hydrogen in the molecular cloud. We use the energy loss function for protons in H_2 as given by Padovani et al.[57] and shown in Figure 4. As explained below, the attenuated spectrum can be written analytically in terms of the Galactic spectrum $j(E)$ and the energy loss function.

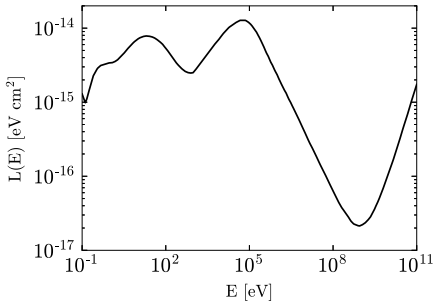

Figure 4. Energy loss function for protons interacting with H_2. Data from ref 57.

The column density of molecular hydrogen, $N(H_2) = \int n(H_2)dl$, can also be expressed in terms of the energy loss function using eq 3 as

$$N(\mathrm{H}_2) = -\int_{E_0}^{E} \frac{dE'}{L(E')} = n(\mathrm{H}_2)[R(E_0) - R(E)] \tag{4}$$

We have introduced the range $R(E)$ of a proton of energy E, defined by

$$R(E) = \frac{1}{n(\mathrm{H}_2)}\int_0^E \frac{dE'}{L(E')} \tag{5}$$

and note that the energy of a proton decreases from E_0 to E after interacting with a column density $N(H_2)$.

Our goal is to compute $j(E, N)$, the Galactic CR proton spectrum after traversing a column density N, in terms of the interstellar spectrum $j(E_0, 0)$ and the energy loss function $L(E)$ by following the prescription of Takayanagi[58] and further elaborated by Padovani et al.[54] We assume that the number of CR protons is conserved, so that

$$j(E, N)dE = j(E_0,0)dE_0 \tag{6}$$

The total differential of eq 4 is given by

$$dN(\mathrm{H}_2) = \frac{\partial N(\mathrm{H}_2)}{\partial E}dE + \frac{\partial N(\mathrm{H}_2)}{\partial E_0}dE_0.$$

If we consider a fixed value of $N(H_2)$, so that $dN(H_2) = 0$, then we find the following relation[c]

$$\frac{dE}{L(E)} = \frac{dE_0}{L(E_0)} \tag{7}$$

Together, eqs 6 and 7 give our desired expression for the attenuated Galactic CR proton spectrum in terms of the Galactic spectrum at the nominal column density $N(H_2) = 0$, for a given value of $N(H_2)$

$$j(E, N) = j(E_0,0)\frac{L(E_0)}{L(E)} \tag{8}$$

All that remains is to determine, for a given $N(H_2)$, the final energy E in the attenuated spectrum for each initial energy E_0 in the interstellar spectrum. For that, we first compute $N(H_2)$ for all values of E and E_0 and then extract contours for a set of $N(H_2)$ values, as shown in Figure 5 ($dN = 0$ along a given contour). Each contour represents a mapping from E_0 to E for a specific column density, which we then fit with the analytic function[54]

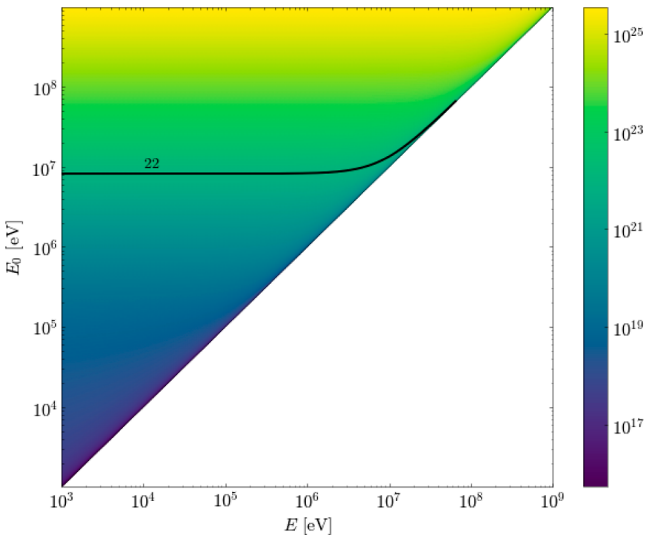

Figure 5. $N(H_2)$ values computed from eq 4 as a function of E_0 and E. The lower right region of the plot is empty because it corresponds to the unphysical situation, $E > E_0$. Overlaid on the plot is a single contour line corresponding to the set of E_0 and E values for which $N(H_2) = 10^{22}$ cm^{-2} (so, $dN = 0$ along the contour).

https://doi.org/10.1021/acsearthspacechem.3c00259
ACS Earth Space Chem. 2024, 8, 79−88

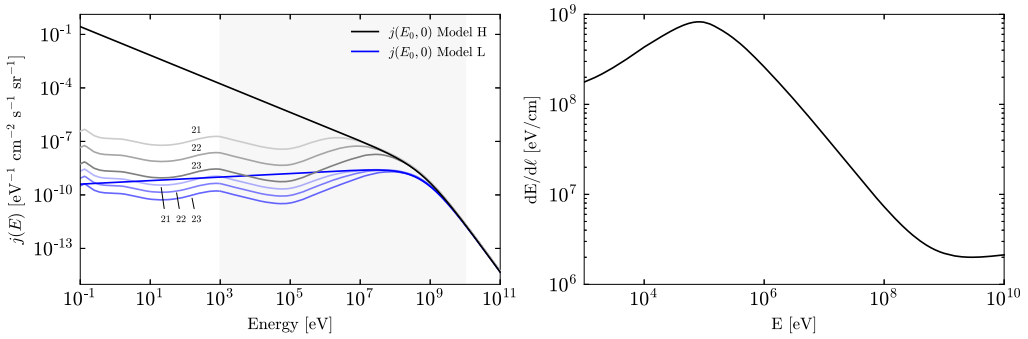

Figure 6. (Left): Interstellar CR proton spectra (black: model H and blue: model L) and attenuated Galactic CR spectra for three column densities, $N(H_2) = 10^{22\pm1}$ cm^{-2} (grayscale: model H and blue-scale: model L). Numbers in the plot indicate $\log_{10}[N(H_2)/\text{cm}^{-2}]$. (Right): Stopping power for protons in liquid water from the NIST PSTAR database.[60] We assume that the stopping power for protons in water ice is approximately the same as that in liquid water. Data are presented as energy loss per path length traveled, assuming a water mass density of 1 g cm^{-3}. Stopping data from NIST are only available for proton energies of 1 keV to 10 GeV, which corresponds to the lightly shaded region in the left-hand plot.

$$E_0(E, N) = \left(cE^b + \frac{N}{N_0}\right)^{1/b} \tag{9}$$

where b, c, and N_0 are fit parameters. Together, eqs 8 and 9 can be used to compute the attenuated Galactic CR spectrum $j(E, N)$ for a given column density $N(H_2)$.

Figure 6 shows the Galactic proton spectra $j(E, 0)$ (for models H and L), along with the attenuated proton spectra $j(E, N)$ for column densities of $N(H_2) = 10^{22\pm1}$ cm^{-2}, consistent with expectations for dark, dense molecular clouds.[d]

Interactions of Protons with Cosmic Ices. Interstellar ices surrounding submicrometer-sized dust grains exist with a broad range of sizes and compositions. Here, we adopt the admittedly simplistic assumption of a sphere of diameter D_{ice} = 100 nm composed entirely of water ice even though interstellar ices contain in lower abundance species such as CO, CO_2, CH_4, and CH_3OH.[61] We further assume that every proton striking the ice sphere will travel through its full diameter D_{ice}. To estimate the energy deposited in the ice by protons, we need to know the stopping power of protons in the ice. Although the precise stopping power dE/dl for protons in ice is not available, for our purposes, it is adequate to use the stopping power of protons in liquid water as a proxy. Those data are available from the NIST PSTAR database[60] and are shown in Figure 6. We further note that most protons in the local CR spectrum lose only a small fraction of their energy in the ice. For example, a 1 MeV proton loses 3 keV of energy over 100 nm (less than 1% of its energy). We, therefore, assign a constant stopping power to each proton as it travels through the ice. As shown in Figure 6, however, the stopping power has a strong energy dependence, which we account for in our analysis by assigning different stopping powers to protons of different initial energies.

We define the secondary electron flux Φ in the ice as the number of secondary electrons per area per time produced in the ice by the attenuated Galactic CR protons

$$\Phi = \frac{2\pi D_{ice}}{w} \int_{E_{min}}^{E_{max}} j(E', N) \left.\frac{dE}{dl}\right|_{E'} dE' \tag{10}$$

where D_{ice} is the diameter of the ice grain (here, taken to be 100 nm), the factor of 2π comes from integrating $j(E, N)$ over solid angle (and only considering protons incident on the exterior surface of the ice grain), and the stopping power dE/dl in the integrand is evaluated at each energy of interest E'. The term w is the differential w-value, which specifies the average energy required to make an electron−hole pair in the ice in the case where a small fraction of the energy of the proton is lost in the ice.[e] We discuss more about the w-value below. The integral is carried out over a range of proton energies [E_{min}, E_{max}]. Our analysis is limited to energies for which stopping power data is available: E_{min} = 1 keV and E_{max} = 10 GeV. Ignoring protons with energy outside of this range will necessarily underestimate the number of secondary electrons produced in the ice. But as we will see, we still find that a significant number of secondary electrons are produced inside the ice by the incident attenuated Galactic CR protons.

We are not aware of any measurements or calculations of the w-value for protons in water ice; we make the reasonable assumption that the w-value for protons in liquid water is approximately the same as that for protons in ice. Baek and Grosswendt[62] calculate w for protons in liquid water as a function of proton energy using three different models. All three provide similar results for large proton energies, with the w-values approaching 25−27 eV. Here, we adopt a conservative value of 30 eV.

RESULTS

Our estimates of the low-energy secondary electron flux produced by CR protons within interstellar ices inside dense molecular clouds are shown in Table 2. For model H, we find a flux of 2×10^2 electrons cm^{-2} s^{-1} for a typical column density of $N(H_2) = 10^{22}$ cm^{-2}. For comparison, the accepted dense cloud photon flux incident on interstellar ices is on the order of 10^3 photons cm^{-2} s^{-1} and only 60% of the flux is estimated to

Table 2. Calculated Secondary Electron Flux Φ Produced within Interstellar Ice Mantles inside Dark Dense Molecular Clouds Due to Incident Galactic CR Protons[a]

CR proton spectrum	log $[N(H_2)/\text{cm}^{-2}]$	Φ (e$^-$cm^{-2} s^{-1})
model H	21	500
	22	200
	23	90
model L	21	20
	22	20
	23	10

[a]Data are presented for models H and L and for three representative values of the column density $N(H_2)$. The values of Φ are rounded to one significant figure.

https://doi.org/10.1021/acsearthspacechem.3c00259
ACS Earth Space Chem. 2024, 8, 79−88

be nonionizing.[63,64] Other factors such as the significantly smaller penetration depth of UV photons[f] compared to that of CR protons will diminish the photon flux relative to that of secondary electrons within interstellar ices.

Secondary electrons are also produced within interstellar ices by other interstellar ionizing radiations such as γ rays, X-rays, and vacuum UV photons and by other components of Galactic CRs such as alpha particles and electrons. In addition, in a region similar to that in which our sun may have been born, the CRIR has been found to be three orders of magnitude higher than the typical interstellar value.[35,36] Because of the reasons enumerated above, we take our estimated secondary electron flux as a lower bound to the ionizing radiation-induced secondary electron flux within interstellar ices. Given that electron-induced dissociation processes typically have cross sections higher than those of photons, our order-of-magnitude secondary electron flux calculations suggest that the effects of ionizing-radiation-induced low-energy secondary electrons are at least as significant as those of photons in the interstellar synthesis of prebiotic molecules whose delivery by comets and meteorites likely kick-started life on earth.

Although our calculations are only directly related to submicron-sized interstellar ice particles, our results also have implications for ices in extrasolar and solar planets (e.g., Mars), dwarf planets (e.g., Pluto), moons (e.g., Europa), asteroids (e.g., Ceres), and comets (e.g., 67P/Churyumov−Gerasimenko). For example, given the orders of magnitude higher penetration depth of Galactic CRs compared to UV photons on the Martian surface, low-energy secondary electrons likely dominate in the subsurface Martian radiolysis, which has recently been hypothesized as a possible source of metabolic energy.[65] Galactic CRs penetrate tens of meters below cometary surfaces facilitating radiolysis of cometary nuclei.[66,67] Our calculations indicate that low-energy electrons should dominate chemical modifications in such environs.

In our planned future work, we will undertake a more detailed analysis, which takes into account that energy deposition by high-energy charged particles is a random process that consists of numerous events, with each event transferring a small amount of energy. Our ongoing calculations involve Geant4-DNA (GEometry ANd Tracking 4-DNA), which is an extension of the Geant4 toolkit,[68] to model the passage of particles through matter. These calculations (to be published) will provide us with the total number of low-energy secondary electrons produced by high-energy charged particles and the energy distribution of the secondary electrons. Moreover, the Geant4 calculations yield microscopic information (e.g., the location of ionization) that could be employed to model chemical reactions that follow energy deposition. Nevertheless, given the three orders of magnitude variations in the measured CRIR that determines the ionizing radiation flux incident on interstellar ices, the order-of-magnitude calculations in this work are sufficient to demonstrate the importance of low-energy secondary electrons vis-à-vis nonionizing photons in the extraterrestrial synthesis of complex organic molecules.

CONCLUSIONS

Because of the primacy of low-energy secondary electrons in all radiation chemistry processes, we have studied the potential role of low-energy electrons in astrochemistry. We estimate the flux of Galactic CR-induced secondary electrons in interstellar ices within dark, dense molecular clouds by considering (1) the CR spectra that best reproduce the CRIR in diffuse interstellar clouds, (2) the attenuated CR particle spectra after propagation through dark, dense molecular clouds, and (3) data from the NIST databases, which provide information on the energy loss for charged particles traversing water. The results based on the attenuated Galactic CR spectrum indicate that the flux of low-energy electrons within these interstellar ices is almost as substantial as the flux of UV nonionizing photons incident on ices in dark, dense molecular clouds. In some star-forming regions where the CRIR due to internal high-energy charged particles has been found to be up to three orders of magnitude higher than the typical interstellar values, low-energy secondary electron flux will dominate that of nonionizing photons. Given that low-energy electrons likely have larger reaction cross sections than photons, we argue that astrochemical models should consider the role of low-energy electrons (<20 eV) in energetic ice processing leading to the extraterrestrial synthesis of complex organic molecules. This information is crucial for understanding the processes involved in forming interstellar prebiotic molecules, which may have played a pivotal role in the emergence of life.

AUTHOR INFORMATION

Corresponding Author

James B. R. Battat − *Department of Physics & Astronomy, Wellesley College, Wellesley, Massachusetts 02481, United States;* orcid.org/0000-0003-1236-1228; Email: jbattat@wellesley.edu

Authors

Qin Tong Wu − *Department of Chemistry, Wellesley College, Wellesley, Massachusetts 02481, United States*

Hannah Anderson − *Department of Chemistry, Wellesley College, Wellesley, Massachusetts 02481, United States*

Aurland K. Watkins − *Department of Chemistry, Wellesley College, Wellesley, Massachusetts 02481, United States;* orcid.org/0000-0002-1341-5737

Devyani Arora − *Department of Chemistry, Wellesley College, Wellesley, Massachusetts 02481, United States*

Kennedy Barnes − *Department of Chemistry, Wellesley College, Wellesley, Massachusetts 02481, United States*

Marco Padovani − *INAF—Osservatorio Astrofisico di Arcetri, 50125 Firenze, Italy;* orcid.org/0000-0003-2303-0096

Christopher N. Shingledecker − *Department of Physics & Astronomy, Benedictine College, Atchison, Kansas 66002, United States;* orcid.org/0000-0002-5171-7568

Christopher R. Arumainayagam − *Department of Chemistry, Wellesley College, Wellesley, Massachusetts 02481, United States;* orcid.org/0000-0002-0722-1151

Complete contact information is available at: https://pubs.acs.org/10.1021/acsearthspacechem.3c00259

Notes

The authors declare no competing financial interest.

ACKNOWLEDGMENTS

We thank Amanda Cheng for assistance with figure preparation. J.B.R.B.'s and C.R.A.'s work was supported by a grant from the National Science Foundation (NSF grant number CHE-1955215). C.R.A.'s work was also supported by Wellesley College (Faculty Awards and Brachman Hoffman small grants). Additionally, this research is partially funded by the Gordon and Betty Moore Foundation through grant

GBMF11565 and grant DOI 10.37807/GBMF11565. The Massachusetts Space Grant Consortium supported the work of H.A. and A.K.W. K.B. gratefully acknowledges funding from the Arnold and Mabel Beckman Foundation.

■ ADDITIONAL NOTES

[a]Although reactive cross sections for photons and electrons as a function of incident energy are unavailable, the photon absorption cross sections and electron trapping cross sections (the probability that an electron will be captured and localized) serve as upper limits to photodissociation and dissociative electron attachment cross sections,[20] respectively. For example, the photon absorption cross section for water has a maximum of 5×10^{-18} cm^2 at ∼8.5 eV.[21] In contrast, the electron trapping cross section for condensed water varies from $\sim 3 \times 10^{-16}$ cm^2 near zero electron energy to $\sim 5 \times 10^{-17}$ cm^2 at 10 eV.[22] The aforementioned limited experimental data suggest that reactive cross sections for electrons are likely larger for electrons than photons, at least for water, the main constituent of interstellar and planetary ices.

[b]https://physics.nist.gov/PhysRefData/Star/Text/PSTAR.html.

[c]Notice that $N(H_2)$, as defined in eq 4, is an explicit function of both E_0 and E because those variables appear in the limits of the integral. By the fundamental theorem of calculus, $\partial N/\partial E = -1/L(E)$, and similarly, $\partial N/\partial E_0 = +1/L(E_0)$.

[d]Dense molecular cloud cores are usually defined as those regions where UV photons of the interstellar radiation field are absorbed so that only CRs penetrate the cloud. See, e.g., Table 3.1 of ref 59.

[e]This is distinct from the integral W-value, which applies to particles that fully stop in the medium. In that case, nuclear interactions, which are important at low projectile energy, make $W \geq w$. In the limit of high projectile energy, W approaches w.

[f]In the condensed phase, 5−9 eV photons, those likely responsible for most solid-state photochemistry, have mean free paths comparable to the thickness of interstellar ice. For example, the mean free path of 8.5 eV photons in condensed water is ∼0.06 μm according to calculations based on the photon absorption cross section (5×10^{-18} cm^2) of water ice. Because the ice mantles surrounding cold interstellar grains are ∼0.1 μm, the photon flux will diminish with penetration depth.

■ REFERENCES

(1) Harris, T. D.; Lee, D. H.; Blumberg, M. Q.; Arumainayagam, C. R. Electron-Induced Reactions in Methanol Ultrathin Films Studied by Temperature-Programmed Desorption: A Useful Method to Study Radiation Chemistry. *J. Phys. Chem.* **1995**, *99*, 9530−9535.

(2) Schmidt, F.; Borrmann, T.; Mues, M. P.; Benter, S.; Swiderek, P.; Bredehöft, J. H. Mechanisms of Electron-Induced Chemistry in Molecular Ices. *Atoms* **2022**, *10*, 25.

(3) Esmaili, S.; Bass, A. D.; Cloutier, P.; Sanche, L.; Huels, M. A. Glycine formation in CO_2:CH_4:NH_3 ices induced by 0−70 eV electrons. *J. Chem. Phys.* **2018**, *148*, 164702.

(4) Arumainayagam, C. R.; Garrod, R. T.; Boyer, M. C.; Hay, A. K.; Bao, S. T.; Campbell, J. S.; Wang, J.; Nowak, C. M.; Arumainayagam, M. R.; Hodge, P. J. Extraterrestrial prebiotic molecules: photochemistry vs. radiation chemistry of interstellar ices. *Chem. Soc. Rev.* **2019**, *48*, 2293−2314.

(5) Cronin, J. W.; Gaisser, T. K.; Swordy, S. P. Cosmic Rays at the Energy Frontier. *Sci. Am.* **1997**, *276*, 44−49.

(6) Altwegg, K.; Balsiger, H.; Bar-Nun, A.; Berthelier, J. J.; Bieler, A.; Bochsler, P.; Briois, C.; Calmonte, U.; Combi, M. R.; Cottin, H.; et al. Prebiotic chemicals-amino acid and phosphorus in the coma of comet 67P/Churyumov-Gerasimenko. *Sci. Adv.* **2016**, *2*, No. e1600285.

(7) Oba, Y.; Takano, Y.; Furukawa, Y.; Koga, T.; Glavin, D. P.; Dworkin, J. P.; Naraoka, H. Identifying the wide diversity of extraterrestrial purine and pyrimidine nucleobases in carbonaceous meteorites. *Nat. Commun.* **2022**, *13*, 2008.

(8) Rivilla, V. M.; Jiménez-Serra, I.; Martín-Pintado, J.; Colzi, L.; Tercero, B.; de Vicente, P.; Zeng, S.; Martín, S.; de la Concepción, J. G.; Bizzocchi, L.; Melosso, M.; Rico-Villas, F.; Requena-Torres, M. A. Molecular Precursors of the RNA-World in Space: New Nitriles in the G+0.693−0.027 Molecular Cloud. *Front. Astron. Space Sci.* **2022**, *9*, 876870.

(9) Theulé, P.; Duvernay, F.; Danger, G.; Borget, F.; Bossa, J. B.; Vinogradoff, V.; Mispelaer, F.; Chiavassa, T. Thermal reactions in interstellar ice: A step towards molecular complexity in the interstellar medium. *Adv. Space Res.* **2013**, *52*, 1567−1579.

(10) Linnartz, H.; Ioppolo, S.; Fedoseev, G. Atom addition reactions in interstellar ice analogues. *Int. Rev. Phys. Chem.* **2015**, *34*, 205−237.

(11) Wayne, R. P. *Principles and Applications of Photochemistry*; Oxford University Press, 1988.

(12) Arumainayagam, C. R. Photochemistry. In *Encyclopedia of Astrobiology*; Springer Nature, 2022, pp 1−6.

(13) Cooper, W. J.; Curry, R. D.; O'Shea, K. E. *Environmental Applications of Ionizing Radiation*, 1st ed.; Wiley, 1998.

(14) Arumainayagam, C. R. Radiation Chemistry. In *Encyclopedia of Astrobiology*; Springer Nature, 2022, pp 1−6.

(15) Pimblott, S. M.; LaVerne, J. A. Production of low-energy electrons by ionizing radiation. *Radiat. Phys. Chem.* **2007**, *76*, 1244−1247.

(16) Arumainayagam, C. R.; Lee, H.-L.; Nelson, R. B.; Haines, D. R.; Gunawardane, R. P. Low-energy electron-induced reactions in condensed matter. *Surf. Sci. Rep.* **2010**, *65*, 1−44.

(17) Klar, D.; Ruf, M.-W.; Hotop, H. Dissociative electron attachment to CCl_4 molecules at low electron energies with meV resolution. *Int. J. Mass Spectrom.* **2001**, *205*, 93−110.

(18) Fabrikant, I. I.; Hotop, H. Low-energy behavior of exothermic dissociative electron attachment. *Phys. Rev. A* **2001**, *63*, 022706.

(19) Marchione, D.; Rosu-Finsen, A.; Taj, S.; Lasne, J.; Abdulgalil, A. G. M.; Thrower, J. D.; Frankland, V. L.; Collings, M. P.; McCoustra, M. R. S. Surface Science Investigations of Icy Mantle Growth on Interstellar Dust Grains in Cooling Environments. *ACS Earth Space Chem.* **2019**, *3*, 1915−1931.

(20) Bass, A. D.; Sanche, L. Absolute and effective cross-sections for low-energy electron-scattering processes within condensed matter. *Radiat. Environ. Biophys.* **1998**, *37*, 243−257.

(21) Cruz-Diaz, G. A.; Caro, G. M. M.; Chen, Y.-J.; Yih, T.-S. Vacuum-UV spectroscopy of interstellar ice analogs. *Astron. Astrophys.* **2014**, *562*, A119.

(22) Simpson, W. C.; Orlando, T. M.; Parenteau, L.; Nagesha, K.; Sanche, L. Dissociative electron attachment in nanoscale ice films: Thickness and charge trapping effects. *J. Chem. Phys.* **1998**, *108*, 5027−5034.

(23) Kaplan, I. G.; Miterev, A. M. *Advances in Chemical Physics*; John Wiley & Sons, Ltd, 1987, pp 255−386.

(24) Gao, Y.; Zheng, Y.; Sanche, L. Low-Energy Electron Damage to Condensed-Phase DNA and Its Constituents. *Int. J. Mol. Sci.* **2021**, *22*, 7879.

(25) Cobut, V.; Frongillo, Y.; Patau, J. P.; Goulet, T.; Fraser, M. J.; Jay-Gerin, J. P. Monte Carlo simulation of fast electron and proton tracks in liquid water - I. Physical and physicochemical aspects. *Radiat. Phys. Chem.* **1998**, *51*, 229−243.

(26) Rezaee, M.; Hill, R. P.; Jaffray, D. A. The Exploitation of Low-Energy Electrons in Cancer Treatment. *Radiat. Res.* **2017**, *188*, 123−143.

(27) Khosravifarsani, M.; Ait-Mohand, S.; Paquette, B.; Sanche, L.; Guérin, B. Design, Synthesis, and Cytotoxicity Assessment of [64Cu]Cu-NOTA-Terpyridine Platinum Conjugate: A Novel Chemoradiotherapeutic Agent with Flexible Linker. *Nanomaterials* **2021**, *11*, 2154.

(28) Pronschinske, A.; Pedevilla, P.; Murphy, C. J.; Lewis, E. A.; Lucci, F. R.; Brown, G.; Pappas, G.; Michaelides, A.; Sykes, E. C. H. Enhancement of low-energy electron emission in 2D radioactive films. *Nat. Mater.* **2015**, *14*, 904−907.
(29) Bespalov, I.; Zhang, Y.; Haitjema, J.; Tromp, R. M.; van der Molen, S. J.; Brouwer, A. M.; Jobst, J.; Castellanos, S. Key Role of Very Low Energy Electrons in Tin-Based Molecular Resists for Extreme Ultraviolet Nanolithography. *ACS Appl. Mater. Interfaces* **2020**, *12*, 9881−9889.
(30) de Vera, P.; Azzolini, M.; Sushko, G.; Abril, I.; Garcia-Molina, R.; Dapor, M.; Solov'yov, I. A.; Solov'yov, A. V. Multiscale simulation of the focused electron beam induced deposition process. *Sci. Rep.* **2020**, *10*, 20827.
(31) Mason, N. J.; Field, D. *Low-Energy Electrons*, 1st ed.; Jenny Stanford Publishing, 2019; pp 371−406.
(32) Shingledecker, C. N.; Vasyunin, A.; Herbst, E.; Caselli, P. On Simulating the Proton-irradiation of O_2 and H_2O Ices Using Astrochemical-type Models, with Implications for Bulk Reactivity. *Astrophys. J.* **2019**, *876*, 140.
(33) Irvine, W. M. *Chemistry in Space*; Springer Netherlands, 1991, pp 89−121.
(34) Boamah, M. D.; Sullivan, K. K.; Shulenberger, K. E.; Soe, C. M.; Jacob, L. M.; Yhee, F. C.; Atkinson, K. E.; Boyer, M. C.; Haines, D. R.; Arumainayagam, C. R. Low-energy electron-induced chemistry of condensed methanol: Implications for the interstellar synthesis of prebiotic molecules. *Faraday Discuss.* **2014**, *168*, 249−266.
(35) Fontani, F.; Ceccarelli, C.; Favre, C.; Caselli, P.; Neri, R.; Sims, I. R.; Kahane, C.; Alves, F. O.; Balucani, N.; Bianchi, E.; et al. Seeds of Life in Space (SOLIS): I. Carbon-chain growth in the Solar-type protocluster OMC2-FIR4. *Astron. Astrophys.* **2017**, *605*, A57.
(36) Ceccarelli, C.; Dominik, C.; López-Sepulcre, A.; Kama, M.; Padovani, M.; Caux, E.; Caselli, P. Herschel finds evidence for stellar wind particles in a protostellar envelope: is this what happened to the young sun? *Astrophys. J. Lett.* **2014**, *790*, L1.
(37) Drury, L. O. Review Article: An introduction to the theory of diffusive shock acceleration of energetic particles in tenuous plasmas. *Rep. Prog. Phys.* **1983**, *46*, 973−1027.
(38) Kirk, J. G.. In *Plasma Astrophysics*; Benz, A. O., Courvoisier, T. J.-L., Eds.; Springer Berlin Heidelberg: Berlin, Heidelberg, 1994, pp 225−314.
(39) Padovani, M.; Hennebelle, P.; Marcowith, A.; Ferrière, K. Cosmic-ray acceleration in young protostars. *A&A* **2015**, *582*, L13.
(40) Padovani, M.; Marcowith, A.; Hennebelle, P.; Ferrière, K. Protostars: Forges of cosmic rays? *A&A* **2016**, *590*, A8.
(41) Rodríguez-Kamenetzky, A.; Carrasco-González, C.; Araudo, A.; Romero, G. E.; Torrelles, J. M.; Rodríguez, L. F.; Anglada, G.; Martí, J.; Perucho, M.; Valotto, C. The Highly Collimated Radio Jet of HH 80−81: Structure and Nonthermal Emission. *Astrophys. J.* **2017**, *851*, 16 Publisher: The American Astronomical Society.
(42) Ainsworth, R. E.; Scaife, A. M. M.; Ray, T. P.; Taylor, A. M.; Green, D. A.; Buckle, J. V. Tentative evidence for relativistic electrons generated by the jet of the young Sun-like star DG Tau. *Astrophys. J. Lett.* **2014**, *792*, L18 Publisher: The American Astronomical Society.
(43) Cabedo, V.; Maury, A.; Girart, J. M.; Padovani, M.; Hennebelle, P.; Houde, M.; Zhang, Q. Magnetically regulated collapse in the B335 protostar?—II. Observational constraints on gas ionization and magnetic field coupling. *arXiv* **2023**, arXiv:2204.10043. preprint [astro-ph.GA]
(44) Lattanzi, V.; Alves, F. O.; Padovani, M.; Fontani, F.; Caselli, P.; Ceccarelli, C.; López-Sepulcre, A.; Favre, C.; Neri, R.; Chahine, L.; Vastel, C.; Evans, L. SOLIS - XVII. Jet candidate unveiled in OMC-2 and its possible link to the enhanced cosmic-ray ionisation rate. *arXiv* **2023**, arXiv:2301.10267. preprint [astro-ph.GA]
(45) Gaisser, T. K.; Engel, R.; Resconi, E. *Cosmic Rays and Particle Physics*, 2nd ed.; Cambridge University Press, 2016.
(46) Stanev, T. *High Energy Cosmic Rays; Astrophysics and Space Science Library*; Springer International Publishing: Cham, Germany, 2021; Vol. *462*.
(47) Accardo, L.; Aguilar, M.; Aisa, D.; Alpat, B.; Alvino, A.; Ambrosi, G.; Andeen, K.; Arruda, L.; Attig, N.; Azzarello, P.; et al. High Statistics Measurement of the Positron Fraction in Primary Cosmic Rays of 0.5−500 GeV with the Alpha Magnetic Spectrometer on the International Space Station. *Phys. Rev. Lett.* **2014**, *113*, 121101.
(48) Aguilar, M.; Aisa, D.; Alpat, B.; Alvino, A.; Ambrosi, G.; Andeen, K.; Arruda, L.; Attig, N.; Azzarello, P.; Bachlechner, A.; et al. Precision Measurement of the Proton Flux in Primary Cosmic Rays from Rigidity 1 GV to 1.8 TV with the Alpha Magnetic Spectrometer on the International Space Station. *Phys. Rev. Lett.* **2015**, *114*, 171103.
(49) Putze, A.; Maurin, D.; Donato, F. p. He, and C to Fe cosmic-ray primary fluxes in diffusion models: Source and transport signatures on fluxes and ratios. *Astron. Astrophys.* **2011**, *526*, A101.
(50) Indriolo, N.; Fields, B. D.; McCall, B. J. The implications of a high cosmic-ray ionization rate in diffuse interstellar clouds. *Astrophys. J.* **2009**, *694*, 257−267.
(51) Cummings, A. C.; Stone, E. C.; Heikkila, B. C.; Lal, N.; Webber, W. R.; Jóhannesson, G.; Moskalenko, I. V.; Orlando, E.; Porter, T. A. Galactic Cosmic Rays in the Local Interstellar Medium: Voyager 1 Observations and Model Results. *Astrophys. J.* **2016**, *831*, 18.
(52) Stone, E. C.; Cummings, A. C.; Heikkila, B. C.; Lal, N. Cosmic ray measurements from Voyager 2 as it crossed into interstellar space. *Nat. Astron.* **2019**, *3*, 1013−1018.
(53) Ivlev, A. V.; Padovani, M.; Galli, D.; Caselli, P. Interstellar dust charging in dense molecular clouds: cosmic ray effects. *Astrophys. J.* **2015**, *812*, 135.
(54) Padovani, M.; Ivlev, A. V.; Galli, D.; Caselli, P. Cosmic-ray ionisation in circumstellar discs. *Astron. Astrophys.* **2018**, *614*, A111.
(55) Indriolo, N.; McCall, B. J. Investigating the Cosmic-Ray Ionization Rate in the Galactic Diffuse Interstellar Medium through Observations of H_3^+. *Astrophys. J.* **2012**, *745*, 91.
(56) Wilms, J.; Allen, A.; McCray, R. On the Absorption of X-Rays in the Interstellar Medium. *Acta Pathol. Jpn.* **2000**, *542*, 914−924.
(57) Padovani, M.; Galli, D.; Glassgold, A. E. Cosmic-ray ionization of molecular clouds. *Astron. Astrophys.* **2009**, *501*, 619−631.
(58) Takayanagi, K. Molecule Formation in Dense Interstellar Clouds. *Publ. Astron. Soc. Jpn.* **1973**, *25*, 327.
(59) Stahler, S. W.; Palla, F. *The Formation of Stars*; Wiley, 2004.
(60) National Institute of Standards and Technology. PSTAR, 2023. https://physics.nist.gov/PhysRefData/Star/Text/PSTAR.html (accessed August 1, 2023).
(61) Öberg, K. I. Photochemistry and Astrochemistry: Photochemical Pathways to Interstellar Complex Organic Molecules. *Chem. Rev.* **2016**, *116*, 9631−9663.
(62) Baek, W. Y.; Grosswendt, B. W values of protons in liquid water. *Radiat. Prot. Dosim.* **2007**, *126*, 93−96.
(63) Prasad, S. S.; Tarafdar, S. P. UV radiation field inside dense clouds - Its possible existence and chemical implications. *Astrophys. J.* **1983**, *267*, 603.
(64) Arumainayagam, C. R.; Herbst, E.; Heays, A. N.; Mullikin, E.; Farrah, M.; Mavros, M. G.. In *Prebiotic Photochemistry: From Urey−Miller-Like Experiments to Recent Findings*; Saija, F., Cassone, G., Eds.; Royal Society of Chemistry, 2021.
(65) Atri, D. Investigating the biological potential of galactic cosmic ray-induced radiation-driven chemical disequilibrium in the Martian subsurface environment. *Sci. Rep.* **2020**, *10*, 11646.
(66) Gronoff, G.; Maggiolo, R.; Cessateur, G.; Moore, W. B.; Airapetian, V.; De Keyser, J.; Dhooghe, F.; Gibbons, A.; Gunell, H.; Mertens, C. J.; Rubin, M.; Hosseini, S. The Effect of Cosmic Rays on Cometary Nuclei. I. Dose Deposition. *Astrophys. J.* **2020**, *890*, 89.
(67) Maggiolo, R.; Gronoff, G.; Cessateur, G.; Moore, W. B.; Airapetian, V. S.; De Keyser, J.; Dhooghe, F.; Gibbons, A.; Gunell, H.; Mertens, C. J.; Rubin, M.; Hosseini, S. The Effect of Cosmic Rays on Cometary Nuclei. II. Impact on Ice Composition and Structure. *Astrophys. J.* **2020**, *901*, 136.
(68) Allison, J.; Amako, K.; Apostolakis, J.; Arce, P.; Asai, M.; Aso, T.; Bagli, E.; Bagulya, A.; Banerjee, S.; Barrand, G.; et al. Recent

developments in Geant4. *Nucl. Instrum. Methods Phys. Res. Sect. A Accel. Spectrom. Detect. Assoc. Equip.* **2016**, *835*, 186−225.

https://doi.org/10.1021/acsearthspacechem.3c00259
ACS Earth Space Chem. 2024, 8, 79−88